JB Journals.ASM.org

The Putative Enoyl-Coenzyme A Hydratase DspI Is Required for Production of the *Pseudomonas aeruginosa* Biofilm Dispersion Autoinducer *cis*-2-Decenoic Acid

Diana T. Amari, Cláudia N. H. Marques, David G. Davies

Department of Biological Sciences, State University of New York at Binghamton, Binghamton, New York, USA

In the present study, we report the identification of a putative enoyl-coenzyme A (CoA) hydratase/isomerase that is required for synthesis of the biofilm dispersion autoinducer *cis*-2-decenoic acid in the human pathogen *Pseudomonas aeruginosa*. The protein is encoded by PA14_54640 (PA0745), named *dspI* for *d*ispersion *i*nducer. The gene sequence for this protein shows significant homology to RpfF in *Xanthomonas campestris*. Inactivation of *dspI* was shown to abolish biofilm dispersion autoinduction in continuous cultures of *P. aeruginosa* and resulted in biofilms that were significantly greater in thickness and biomass than those of the parental wild-type strain. Dispersion was shown to be inducible in *dspI* mutants by the exogenous addition of synthetic *cis*-2-decenoic acid or by complementation of Δ*dspI in trans* under the control of an arabinose-inducible promoter. Mutation of *dspI* was also shown to abolish *cis*-2-decenoic acid production, as revealed by gas chromatography-mass spectrometry (GC-MS) analysis of cell-free spent culture medium. The transcript abundance of *dspI* correlated with cell density, as determined by quantitative reverse transcriptase (RT) PCR. This regulation is consistent with the characterization of *cis*-2-decenoic acid as a cell-to-cell communication molecule that regulates biofilm dispersion in a cell density-dependent manner.

Biofilm dispersion is the terminal stage of the biofilm developmental cycle, where bacteria regulate their escape from a biofilm and transition to a mobile planktonic lifestyle (1, 2). Induction of biofilm dispersion in *Pseudomonas aeruginosa* occurs naturally when biofilm microcolonies attain a critical size, releasing bacteria as free cells into the surrounding environment (2, 3). Recently, we have reported that the small messenger fatty acid molecule *cis*-2-decenoic acid (*cis*-DA), produced by *P. aeruginosa* in batch and continuous cultures, acts as the autoinducer of biofilm dispersion for *P. aeruginosa* (3). This molecule has also been shown to induce biofilm dispersion in a range of Gram-negative and Gram-positive bacteria and in the fungal pathogen *Candida albicans* (3).

The autoinducer *cis*-DA is a fatty acid cell-to-cell communication molecule with structural homology to *cis*-11-methyl-2-dodecenoic acid (DSF), isolated from *Xanthomonas campestris* (4, 5). Analogs of DSF have been identified in *Burkholderia cenocepacia* (*cis*-2-dodecenoic acid [BDSF]), *Streptococcus mutans* (*trans*-2-decenoic acid [SDSF]), and *Xylella fastidiosa* (*trans*-2-tetradecenoic acid [*Xy*DSF]) (6–8). Additional, structurally related fatty acid signals have been identified in the genera *Burkholderia*, *Xanthomonas*, and *Stenotrophomonas* (6, 8–13). Fatty acid signals have been shown to regulate a wide range of bacterial behaviors, including virulence, motility, biofilm development, and dispersion (4, 8–10, 12, 14–23).

The mechanism of fatty acid signal biosynthesis appears to be widely conserved. DSF biosynthesis in *X. campestris* is dependent on the gene *rpfF*, which encodes a putative enoyl-coenzyme A (CoA) hydratase (4, 24). The role of RpfF homologs in fatty acid signal biosynthesis has subsequently been established in *B. cenocepacia* (6), *Xanthomonas oryzae* pv. *oryzae* (10), *X. fastidiosa* (18), *Stenotrophomonas maltophilia* (13), and *Xanthomonas axonopodis* pv. *glycines* (20).

In the present work, we report that the gene PA14_54640 (PA0745), named *dspI* (*d*ispersion *i*nducer), is required for production of the dispersion-inducing cell-to-cell signal *cis*-DA, synthesized by *P. aeruginosa*. The gene *dspI* encodes a putative enoyl-CoA hydratase/isomerase responsible for catalyzing the formation of α,β-unsaturated fatty acids. We further demonstrate that expression of *dspI* is correlated with cell density during planktonic and biofilm growth.

MATERIALS AND METHODS

Bacterial strains, plasmids, media, and culture conditions. All bacterial strains and plasmids used in this study are listed in Table 1. *P. aeruginosa* strain PA14 was used as a parental strain for all work in the present study. Planktonic cultures were grown aerobically at 22°C in modified EPRI medium containing 0.005% ammonium nitrate, 0.00019% KH_2PO_4, 0.00063% K_2HPO_4 (pH 7.0), and 0.001% Hutner salts (25) supplemented with 0.2% glucose or in Luria-Bertani (LB) broth (BD, Sparks, MD) in flasks with shaking at 220 rpm. Continuous-culture biofilms were grown at 22°C in modified EPRI medium or 5% LB broth in tube reactors. Semibatch culture biofilms were grown in 20% LB broth in 24-well culture plates. Gene complementation experiments were performed in modified EPRI medium or 5% LB broth with or without 0.1% arabinose. Antibiotics were used at the following concentrations: 75 μg/ml gentamicin (Gm), 250 μg/ml carbenicillin (Cb), and 50 μg/ml tetracycline (Tet) for *P. aeruginosa*; 50 μg/ml ampicillin (Amp), 25 μg/ml kanamycin (Km), and 20 μg/ml Tet for *E. coli*. Cb at a concentration of 10 μg/ml was used for maintenance of the pMJT1 plasmid in *P. aeruginosa* continuous-culture biofilm reactors.

Received 14 June 2013 Accepted 1 August 2013

Published ahead of print 9 August 2013

Address correspondence to David G. Davies, dgdavies@binghamton.edu.

Supplemental material for this article may be found at http://dx.doi.org/10.1128/JB.00707-13.

doi:10.1128/JB.00707-13

TABLE 1 Bacterial strains and plasmids

Strain or plasmid	Description	Reference or source
Strains		
E. coli		
DH5α	λ$^-$ ϕ80d*lacZ*ΔM15 Δ(*lacZYA-argF*)*U169 recA1 endA1 hsdR17*(r_K^- m_K^-) *supE44 thi-1 gyrA relA1*	Invitrogen Corp.
P. aeruginosa PA14		
PA14	Wild type	26
PA14Δ19740	PA14 19740::MAR2 × T7; Gm^r	26
PA14Δ26690	PA14 26690::MAR2 × T7; Gm^r	26
PA14Δ28310	PA14 28310::MAR2 × T7; Gm^r	26
PA14Δ40640	PA14 40640::MAR2 × T7; Gm^r	26
PA14Δ40980	PA14 40980::MAR2 × T7; Gm^r	26
PA14Δ43440	PA14 43440::MAR2 × T7; Gm^r	26
PA14Δ51110	PA14 51110::MAR2 × T7; Gm^r	26
PA14Δ*dspI*	PA14 54640::MAR2 × T7; Gm^r	26
PA14Δ*dspI*/pMJT	PA14 Δ*dspI* bearing empty pMJT-1 vector; Gm^r Cb^r	This study
PA14Δ*dspI*/pMJT-*dspI*	Complementation of Δ*dspI*; Gm^r Carb^r; arabinose inducible	This study
PA14/*dspI-lacZ*	pCTX-*dspI-lacZ* conjugated into PA14; Tet^r	This study
PA14/*lacZ*	pCTX conjugated into PA14; Tet^r	This study
Plasmids		
pCR2.1-TOPO	TA cloning vector; Km^r Amp^r	Invitrogen Corp.
pRK2013	Helper plasmid for triparental mating; *mob tra*; Km^r	31
pMJT1	*araC*-P_{BAD} casette of pJN105 cloned into pUCP18; Amp^r Cb^r	27
pCTX	mini-CTX-*lacZ*; Tet^r	28
pMJT-*dspI*	*dspI* cloned into pMJT1 using primers dspI_NheI_for/dspI_SacI_rev; Cb^r	This study
pCTX-*dspI-lacZ*	*dspI* promoter reporter construct in mini-CTX-*lacZ* using primers dspI-PROM_XhoI_for/dspI-PROM_EcoRI_rev; Tet^r	This study

Strain construction. Complementation of Δ*dspI* (26) was accomplished by placing the gene under the control of an arabinose-inducible P_{BAD} promoter in the pMJT1 vector (27). Briefly, the open reading frame of *dspI* was amplified by PCR using primers listed in Table S1 in the supplemental material and cloned into pMJT1 at restriction sites indicated in Table S1. Plasmids were mobilized into *P. aeruginosa* from *E. coli* via electroporation, and transformants were selected by growth on LB medium with 250 μg/ml Cb. Strains were confirmed to contain vector constructs following amplification by PCR using MCS primers for pMJT1 listed in Table S1 in the supplemental material.

Reporter strain construction. A transcriptional reporter for *dspI* was constructed by placing the promoter region of *dspI* upstream of the *lacZ* gene in the mini-CTX-*lacZ* vector (28). We found that *dspI* was cotranscribed with the upstream genes PA14_54620 and PA14_54630 (see Fig. S1 in the supplemental material). A 500-bp region of DNA upstream of the gene PA14_54620 was selected as including the putative promoter region of *dspI* based on the observation that most promoters are between 100 and 200 bp long and recognizing that multiple promoters are possible in *P.* aeruginosa, as is the case for *algD* (29, 30). This sequence was amplified by PCR using primers listed in Table S1 in the supplemental material, cloned into the mini-CTX-*lacZ* vector at restriction sites indicated in Table S1, and introduced into *P. aeruginosa* via triparental mating (31). Transformants were selected by growth on Vogel-Bonner minimal medium (VBMM) containing 0.3% citrate as the sole carbon source (32) and supplemented with Tet. Chromosomal vector integration was confirmed via PCR amplification using primers for the *attB* integration site listed in Table S1.

Dispersion phenotype screen. Biofilms were grown in semi-batch culture on the submerged surfaces of 24-well cell culture plates inoculated with 250 μl/well overnight *P. aeruginosa* culture diluted 1:100 in 20% LB growth medium and incubated at 37°C with shaking at 220 rpm for 24 h. The plates were incubated at a 45° angle to allow biofilm development within each well. The medium in the wells was replaced every 24 h for 6 days to promote biofilm growth and remove planktonic cells. Images of biofilm microcolonies were viewed by transmitted light using an Olympus BX60 microscope and 20× and 50× UPlanF Olympus objectives. Images used to evaluate biofilm dispersion in wild-type and mutant bacterial strains were recorded using a ProgRes CF camera (Jenoptik, Jena, Thuringia, Germany) and processed with ProgRes CapturePro 2.7.7 software.

Microscopic analysis. A continuous-culture once-through flow cell (BioSurface Technologies, Bozeman, MT) was configured to observe biofilm growth, architecture, and development on a glass substratum as described previously (3). Biofilms grown in flow cells were observed by transmitted light as described above. The biofilms were also analyzed by confocal laser scanning microscopy (CLSM) using a Leica TCS SP5 confocal microscope and Syto 40 nucleic acid stain (Invitrogen Corp.). The CLSM images were processed using LAS AF software v. 2.4.1, and quantitative analysis was performed by COMSTAT using MATLab software to determine the biofilm biomass, average thickness, and total thickness (33). All microscopy experiments were performed in triplicate.

Biofilm dispersion assays. *P. aeruginosa* biofilm cultures were grown in continuous-flow tube reactors as described previously (2, 3, 34). Briefly, the interior surfaces of silicone tubing (81.5 cm long by 14-mm inner diameter; Masterflex; Cole Parmer, Inc.) of a continuous-culture once-through reactor system were used to culture biofilms. The tubing was connected to an influent medium reservoir and effluent waste reservoir. Medium was pumped through the closed and sterilized reactor system using an eight-head peristaltic pump (Cole Parmer, Inc.) at a flow rate of 0.2 ml/min. Silicone tubes were inoculated with 6 ml of log-phase cultures of *P. aeruginosa* by syringe through a rubber septum immediately upstream from each reactor tube. Bacterial cells were allowed to attach to the surface of the tubing for 1 h under static conditions prior to initiation of medium flow. Biofilms were grown at 22°C for a period of 6 days.

Biofilm dispersion assays were performed on 6-day biofilm cultures by addition of *cis*-DA or sterile medium under static flow conditions. Synthetic *cis*-DA (310 nM) or sterile medium was added to test or control

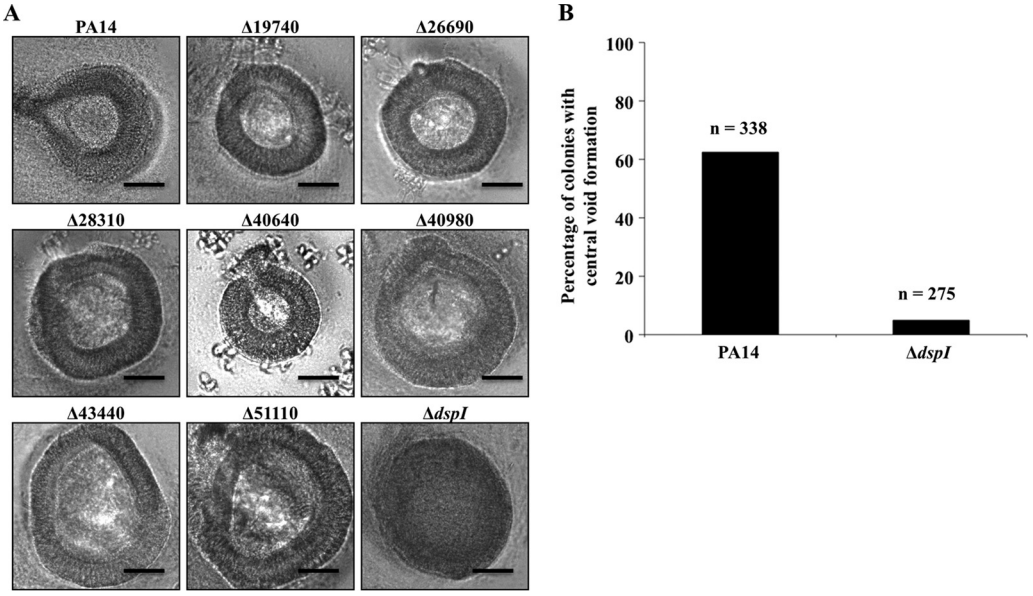

FIG 1 Microcolonies of *P. aeruginosa* PA14 biofilms grown in 24-well cell culture plates demonstrating the native dispersion response. (A) Transmitted-light images showing the presence and absence of interior voids formed within microcolonies of wild-type PA14 and 8 putative enoyl-CoA hydratase mutants. Biofilms of the *dspI* (PA14_54640) mutant showed no evidence of void formation. All images are shown at the same relative size at ×200 magnification. Scale bars, 50 μm. (B) Quantification of microcolony voids formed as a percentage of the total number of microcolonies observed for biofilms of PA14 and Δ*dspI* strains.

tubes, respectively, via a rubber septum upstream of the biofilm reactor. Following a 2-h incubation, both the liquid fraction, containing released bacterial cells, and the remaining biofilm from each tube were collected separately on ice. CFU were determined by serial dilution and plating. Dispersion efficacy was calculated as follows: dispersion efficacy = (CFU in liquid fraction × 100)/(CFU in liquid fraction + CFU in biofilm fraction).

Preparation of spent medium. Preparation of cell-free spent culture medium was performed as described previously (3) with the following modifications. Batch cultures of *P. aeruginosa* wild type PA14 or the *dspI* mutant were grown in 4 liters of modified EPRI medium for 10 days at 22°C with stirring at 220 rpm. Batch cultures of *P. aeruginosa* Δ*dspI*/pMJT-*dspI* or Δ*dspI*/pMJT were grown in 4 liters of arabinose-supplemented LB medium for 10 days at 22°C with stirring at 220 rpm. Cell-free spent culture medium was prepared by centrifugation (16,000 × *g*; 20 min; 4°C), followed by prefiltration using a 0.45-μm nitrile filter (Millipore, Billerica, MA) and secondary filtration using a 0.2-μm syringe filter (Millipore). The cell-free spent culture medium was stored at 4°C.

Preparation of CSM. Chloroform-extracted spent-medium (CSM) samples were prepared as described previously (3) with the following modifications. The organic compounds contained in 3 liters of spent medium were extracted in 0.96 liters of chloroform. The chloroform was evaporated using a Rotavapor R-3000 rotovap (Buchi, Switzerland), and the remaining organic material was resuspended in 2 ml of 18 mΩ water. The CSM contained a final concentration of *cis*-DA 250-fold greater than in cell-free spent culture medium.

GC-MS. Preparation of CSM and synthetic *cis*-DA (Carbosynth Limited, Compton-Berkshire, United Kingdom) samples for gas chromatography-mass spectrometry (GC-MS) and tandem mass spectrometry (MS-MS) analyses was carried out as previously described (3). Spectra were obtained with a Shimadzu (Columbia, MD) QP5050A GC-MS system, and analysis was performed using the Lab Solutions program GC-MS Solution (version 1.2).

Batch culture growth curve. To determine cell density throughout planktonic growth, a growth curve of *P. aeruginosa* PA14 was performed on cultures grown in shake flasks at 23°C. Overnight cultures were grown in LB broth, optical density at 600 nm (OD_{600}) adjusted, and diluted 1:100 in fresh LB broth. Absorbance readings (OD_{600}) were taken at 12 time points throughout 32 h of growth. Experiments were carried out in triplicate with independent overnight cultures.

qRT-PCR. Quantitative reverse transcriptase PCR (qRT-PCR) was used to determine the expression levels of *dspI* using 1 μg of total RNA isolated from wild-type *P. aeruginosa* cells grown as planktonic cultures (6.5 h, 10 h, 12.5 h, 15 h, and 24 h) and as biofilm cultures (1-, 3-, and 5-day cultures). qRT-PCR was also used to determine the effect of the exogenous addition of 310 nM *cis*-DA on *dspI* transcript abundance in 12.5-h-old PA14 planktonic cultures. Isolation of mRNA and subsequent cDNA synthesis were performed as described previously (35–38). Transcript amplification by qRT-PCR was performed according to the manufacturer's specifications with an Eppendorf Mastercycler ep realplex instrument (Eppendorf AG, Hamburg, Germany) and a KAPA SYBR FAST qPCR Kit (KAPA Biosystems, Woburn, MA), using oligonucleotide primers listed in Table S1 in the supplemental material. The gene *mreB* was used as a housekeeper control. Relative transcript abundances were determined using the ep realplex software (Eppendorf AG). Transcript quantification was normalized (based on the threshold cycle [C_T] value) to *mreB* transcripts, followed by determination of transcript abundance ratios. The fold change in *dspI* abundance for planktonic and biofilm cells was determined relative to *dspI* abundance of early-exponential planktonic samples. Melting curve analyses were performed to ensure specific single-product amplification.

***dspI* transcription assays.** The β-galactosidase specific activities of strains harboring the *dspI* reporter construct were determined using the Miller assay (39) modified to determine specific β-galactosidase activity and normalized to cell protein extracts, as described previously (38, 40). An extinction coefficient of 4,500 nl/nmol/cm for *o*-nitrophenyl-β-galactoside (ONPG) cleavage at 420 nm was used. Specific-activity values were calculated following subtraction of background levels of β-galactosidase activity in a promoterless *lacZ* control strain.

β-Galactosidase activity was also assessed by fluorescence microscopy (2). Microscopic analysis of *dspI* expression during planktonic and biofilm growth was performed for cultures grown in medium containing 0.02 g/liter methylumbelliferyl β-D-galactopyranoside (MUG) dissolved in *N*,*N*-di-methylformamide. β-Galactosidase activity was assessed by mi-

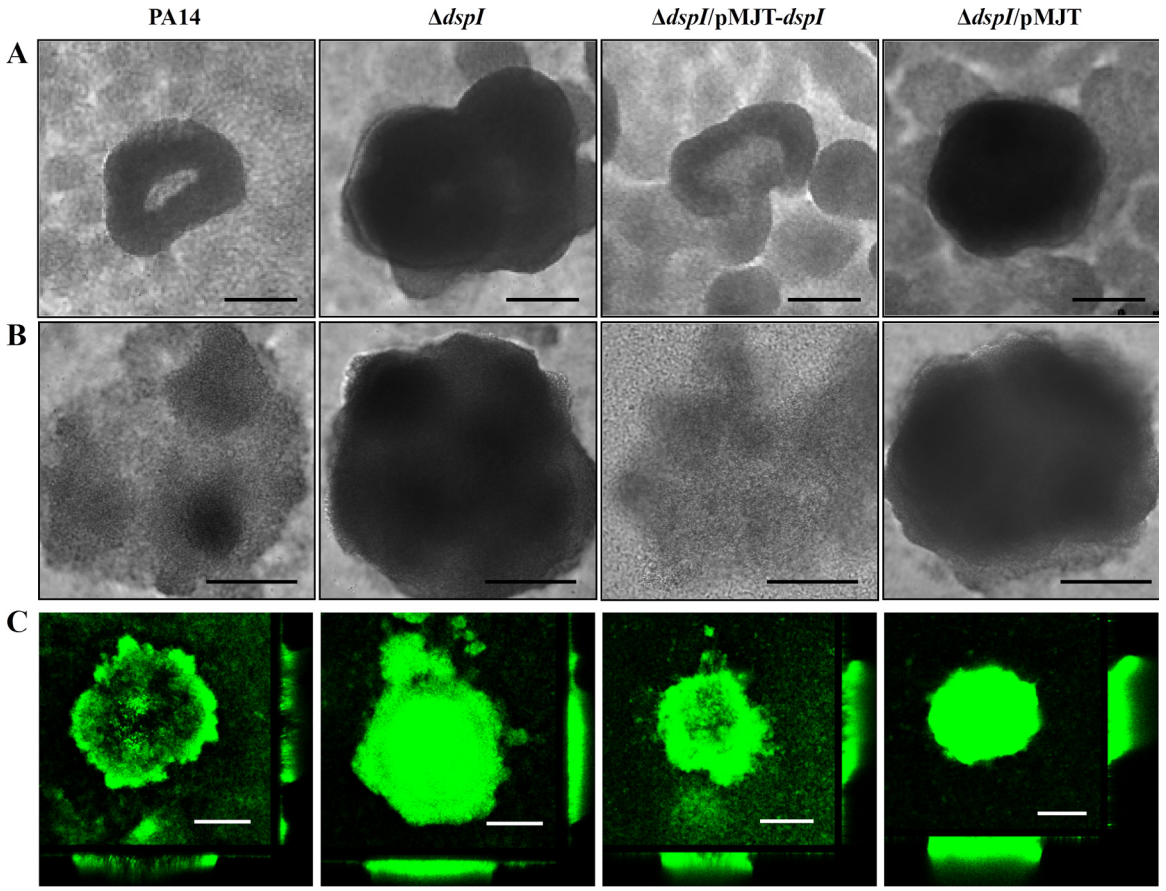

FIG 2 *dspI* is required for native biofilm dispersion. Transmitted-light images (A and B) and confocal laser scanning microscopy images (C) at a magnification of ×500 of *P. aeruginosa* wild-type and *dspI* mutant biofilms. The photomicrographs show microcolonies of biofilms grown in modified EPRI medium (A) or 5% LB medium (B and C) for 6 days, with continuous *dspI* induction in the complemented *dspI* mutant strain. Microcolonies of the *dspI* mutant remained solid, whereas wild-type and complemented mutant biofilms showed dispersion. Experiments were completed in triplicate. Scale bars, 50 μm.

croscopy by examination under long-wave UV excitation (2, 41). Samples were analyzed using an exposure time of 1,500 ms, with UV illumination only during image collection. β-Galactosidase activity was determined for both planktonic (early-exponential, mid-exponential, late-exponential, and early- and late-stationary-phase) and biofilm (1-, 3-, and 5-day) cells grown in batch culture or continuous-culture flow cells, respectively.

Statistical analysis. Student's *t* test was performed for pairwise comparisons of groups, and multivariate analyses were performed using one-way analysis of variance (ANOVA).

RESULTS

Identification of the *P. aeruginosa* fatty acid synthase gene required for native biofilm dispersion. We have previously reported that the cell-to-cell communication molecule *cis*-DA was capable of inducing a biofilm dispersion response in *P. aeruginosa* (3). To identify a key enzyme required for the production of *cis*-DA, we focused on novel enoyl-CoA hydratase proteins with potential to be required for native biofilm dispersion. A query of the *P. aeruginosa* database (www.pseudomonas.com) revealed 15 putative enoyl-CoA hydratases encoded within the genome. Knockout mutations were found to be nonlethal in 8 of these genes (PA14_19740/PA3426, PA14_26690/PA2890, PA14_28310/PA2767, PA14_40640/PA1846, PA14_40980/PA1821, PA14_43440/PA1629, PA14_51110/PA1021, and PA14_54640/PA0745). Transposon mutants of these genes were selected for analysis by dispersion phenotype screening (see Materials and Methods) to determine whether they naturally formed central voids within microcolonies following 6 days of biofilm growth. Central-void formation in biofilm microcolonies is a characteristic consequence of natural dispersion, inducible with endogenously produced *cis*-DA. These voids result from the release of bacteria from the interiors of mature biofilm microcolonies (3, 42). All of the mutants tested, with the exception of PA14_54640/PA0745 (*dspI*), formed a central void in the majority of microcolonies observed by microscopic analysis (Fig. 1A). Void formation was observed in only 5% of microcolonies of *dspI* mutant biofilms compared to 63% of wild-type biofilm microcolonies (Fig. 1B). The presence of void spaces in *dspI* mutant biofilms may have resulted from *P. aeruginosa* dispersion in response to factors other than *cis*-DA. Thus, complete loss of the dispersion phenotype may not be possible with a single mutation. Interestingly, of all the enoyl-CoA hydratase proteins investigated, DspI had the highest homology (5.0E−14) to RpfF, the synthase for DSF in *X. campestris* (4).

***dspI* is required for native biofilm dispersion and is restored by complementation of *dspI* in *trans*.** To further investigate the native dispersion phenotype of *dspI* mutant biofilms, the architecture of 6-day biofilms was analyzed using a microscope-mounted continuous-culture flow cell reactor system. Previous work in our laboratories has shown the dispersion stage of *P. aeruginosa* biofilm development to occur at day 6 under the continuous-culture

TABLE 2 Quantitative analysis of biofilm architecture using COMSTAT[a]

Strain and conditions	Total biomass ($\mu m^3/\mu m^2$)	Avg biofilm thickness (μm)	Maximum biofilm thickness (μm)
Continuous *dspI* induction (5% LB; 6-day-old biofilms)			
PA14	9.4 ± 3.8	13.4 ± 5.0	61.9 ± 21.8
Δ*dspI*	22.0 ± 7.0[c]	35.5 ± 11.5[c]	127.1 ± 35.6[c]
Δ*dspI*/pMJT-*dspI*	6.5 ± 3.9[d,e]	10.4 ± 5.1[d,e]	64.2 ± 23.0[d,e]
Δ*dspI*/pMJT	25.4 ± 10.8[c]	39.3 ± 16.8[c]	97.4 ± 35.7[c]
Before *dspI* induction (EPRI; 5-day-old biofilms)			
PA14	9.3 ± 2.9	9.7 ± 3.4	25.7 ± 7.8
Δ*dspI*	14.8 ± 2.4[c]	16.0 ± 2.6[c]	43.0 ± 14.0[c]
Δ*dspI*/pMJT-*dspI*	14.5 ± 5.6[c,f]	16.4 ± 6.0[c,f]	38.7 ± 18.0[c,f]
Δ*dspI*/pMJT	16.7 ± 3.8[c]	18.3 ± 4.4[c]	38.8 ± 12.1[c]
After *dspI* induction (EPRI; 6-day-old biofilms)[b]			
PA14	9.2 ± 4.7	10.5 ± 5.4	30.23 ± 13.4
Δ*dspI*	20.2 ± 3.5[c]	22.5 ± 3.7[c]	53.8 ± 16.3[c]
Δ*dspI*/pMJT-*dspI*	6.0 ± 3.8[d,e]	7.0 ± 4.3[d,e]	20.4 ± 8.3[d,e]
Δ*dspI*/pMJT	21.8 ± 7.3[c]	23.5 ± 8.1[c]	40.0 ± 12.4[c]

[a] COMSTAT analysis was carried out on biofilms grown in replicate ($n = 2$) from at least 8 images per replicate.
[b] *dspI* expression was induced by growth in arabinose-containing culture medium for 24 h.
[c] Significantly different from the wild-type PA14 ($P < 0.01$), as determined by single-variant ANOVA.
[d] Significantly different from the *dspI* mutant ($P < 0.01$), as determined by single-variant ANOVA.
[e] Not significantly different from the wild type ($P > 0.01$), as determined by single-variant ANOVA.
[f] Not significantly different from the *dspI* mutant ($P > 0.01$), as determined by single-variant ANOVA.

conditions used in this work. We hypothesized that loss of native dispersion by mutation of *dspI* would result in increased biomass and microcolony size of 6-day biofilms compared to the wild type. Both the wild type and the *dspI* mutant formed biofilm microcolonies with distinct three-dimensional architecture; however, the *dspI* mutant biofilm displayed microcolonies with greater thickness and diameter in both modified EPRI and 5% LB media (Fig. 2A and B). Quantitative analysis of biofilm architecture using COMSTAT confirmed these observations, indicating that the *dspI* mutant 6-day biofilms had greater average and maximum thickness, as well as greater total biomass, than the wild-type strain (Table 2).

We investigated whether activation of a plasmid-borne *dspI* gene in Δ*dspI* biofilms would result in restoration of the dispersion phenotype. Complementation of *dspI* for the duration of biofilm development resulted in biofilm architecture not observably different from that of the wild type and restored void formation associated with the natural-dispersion phenotype (Fig. 2A and B and Table 2). To determine the effect of *dspI* induction in mature Δ*dspI* biofilms, *dspI* gene expression was induced between days 5 and 6 in the complemented mutant strain. Quantitative analysis of biofilm architecture using COMSTAT was performed for 5-day (preinduction) biofilms and again for 6-day (postinduction) biofilms for the wild type, *dspI* mutant, and *dspI*-inducible complement grown in flow cell reactors. At 5 days, both the *dspI* mutant and the *dspI* inducible complement formed biofilms with greater average and maximum thickness, as well as greater total biomass, than the wild type. However, at 6 days, induction of *dspI* resulted in biofilms with average and maximum thickness and total biomass more similar to those of wild-type biofilms than those of biofilms of the uninduced *dspI* mutant (Table 2).

Mutation of *dspI* does not impair growth. We tested whether mutation of *dspI* would have an impact on cellular growth rates to ensure that there was no difference in growth between wild-type and mutant strains in the study. Growth curves of both the wild type and the *dspI* mutant were found to be superimposable, indicating no difference in growth kinetics between the two strains (see Fig. S2 in the supplemental material).

Exogenous addition of *cis*-2-decenoic acid restores dispersion in *dspI* mutant biofilms. To investigate whether *dspI* mutants (deficient in native dispersion) disperse in response to exogenous addition of synthetic *cis*-DA, 6-day biofilms grown in

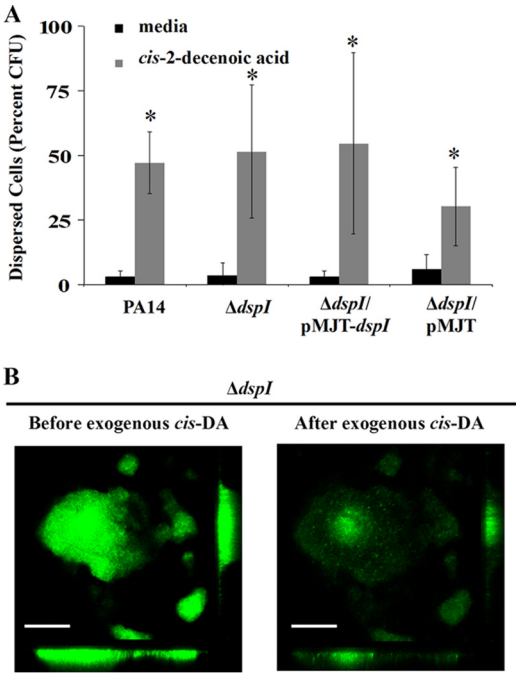

FIG 3 *dspI* mutant biofilms disperse in the presence of exogenous *cis*-DA. (A) Biofilms of wild-type PA14, *dspI* mutants, or complemented *dspI* mutants were grown in continuous-culture tube reactors for 6 days and switched to fresh medium or *cis*-DA for 2 h under static conditions. The numbers of released cells in the bulk liquid of each tube and of the remaining biofilm cells in each tube were determined by viable count (CFU). Percent dispersion was calculated as a function of released cells (CFU) divided by the total number of CFU from each tube (released cells plus remaining biofilm cells). Error bars indicate one standard deviation. (B) CLSM images of mature *dspI* mutant biofilm microcolonies grown in continuous culture in a microscope-mounted flow cell before and after the addition of *cis*-DA. Microcolony disaggregation is shown following treatment under static conditions for 1 h. Control biofilms treated with fresh medium showed no disaggregation (not shown). The images are the same relative size at ×500 magnification. Scale bars, 50 μm. Experiments were completed in triplicate. *, values significantly different from the respective negative control ($P < 0.01$).

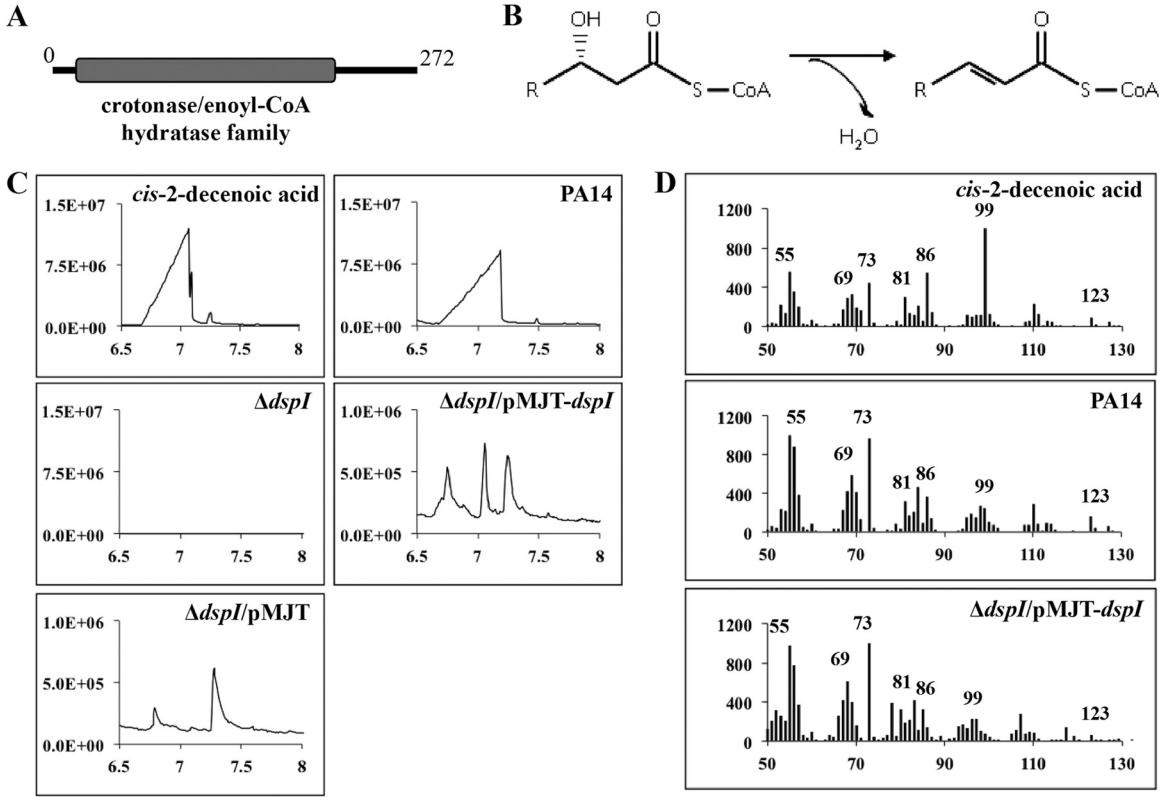

FIG 4 *dspI* is required for synthesis of *cis*-2-decenoic acid in *P. aeruginosa*. (A) DspI contains a conserved domain (gray) belonging to the crotonase/enoyl-CoA hydratase family, which includes many diverse enzymes involved in fatty acid metabolism. (B) The predicted enzymatic reaction performed by the enoyl-CoA hydratase *dspI* includes the formation of a double bond at the β-carbon of small fatty acids. (C) Spectral analysis of synthetic *cis*-DA and CSM prepared from the *P. aeruginosa* PA14 wild type and mutants with *dspI* inactivated or complemented was performed using gas chromatography-mass spectrometry. The *y* axes indicate intensity; the *x* axes indicate time in minutes. (D) MS-MS fragmentation patterns of the 7.0-min peak from the GC-MS spectra of *cis*-DA, PA14 CSM, and CSM of the complemented *dspI* mutant. The *y* axes indicate intensity; the *x* axes indicate *m/z*.

continuous-culture tube reactors were exposed to medium containing synthetic *cis*-DA (310 nM) or carrier control for a period of 2 h. Exogenous addition of *cis*-DA to *dspI* mutant cultures resulted in the release of 51% of the total biofilm population into the bulk liquid. This number is comparable to the release of 47% of biofilm cells by the wild-type strain and 55% by the complemented *dspI* mutant strain. Carrier controls showed 4%, 3%, and 3% cell release, respectively (Fig. 3A). When viewed by CLSM, biofilms of the *dspI* mutant were observed to become significantly reduced in biomass following treatment for 1 h with synthetic *cis*-DA. The results from a representative experiment are shown in Fig. 3B.

***dspI* is essential for production of *cis*-2-decenoic acid.** The *dspI* gene encodes a 272-amino-acid peptide harboring a crotonase/enoyl-CoA hydratase-like conserved domain (www.ncbi.nlm.nih.gov), similar to other enoyl-CoA hydratase/isomerase proteins involved in fatty acid metabolism (Fig. 4A). Enoyl-CoA hydratase/isomerase proteins are known to catalyze the dehydration reaction in short-chain fatty acids, resulting in the formation of a double bond at the 2,3 carbon (Fig. 4B). These proteins are also known to catalyze the *cis*/*trans* isomerization of double bonds. To investigate whether *dspI* mutants produce the *cis*-DA signal, samples of cell-free CSM were chemically analyzed using GC-MS. A single major peak with a retention time of 7.0 min was detected for CSM of the wild type and the complemented *dspI* mutant, identical to that of synthetic *cis*-DA compound, but was absent in the *dspI* mutant (Fig. 4C). The presence of *cis*-DA in the samples was confirmed by MS-MS; the fragmentation patterns for all three peaks were shown to be identical at the 95% confidence interval (Fig. 4D). These findings indicated that *dspI* is required for production of *cis*-DA in *P. aeruginosa* and that DspI is most likely the terminal enzyme in the synthesis pathway, responsible for double-bond formation and *cis*/*trans* isomerization.

Transcription of *dspI* is correlated with cell density during planktonic and biofilm growth. We sought to characterize the transcriptional regulation of *dspI* throughout planktonic and biofilm growth. During planktonic growth, cellular *dspI* transcript abundance was observed to increase throughout the 24-h period of batch growth (Fig. 5A). A 7-fold increase was detected between 10 h and 12.5 h, followed by a 4-fold increase between 12.5 h and 15 h. Finally, a 14-fold increase between 15 h and 24 h was observed (Fig. 5B). Similarly, under biofilm conditions, *dspI* transcript levels increased from 1 to 5 days, with a 5-fold increase between day 1 and day 3 and a 1-fold increase between day 3 and day 5. These findings suggested that expression of *dspI*, under both planktonic and biofilm growth conditions, is correlated with cell density.

A transcriptional reporter for *dspI*. A chromosomal transcriptional *lacZ* fusion for the *dspI* promoter was used to deter-

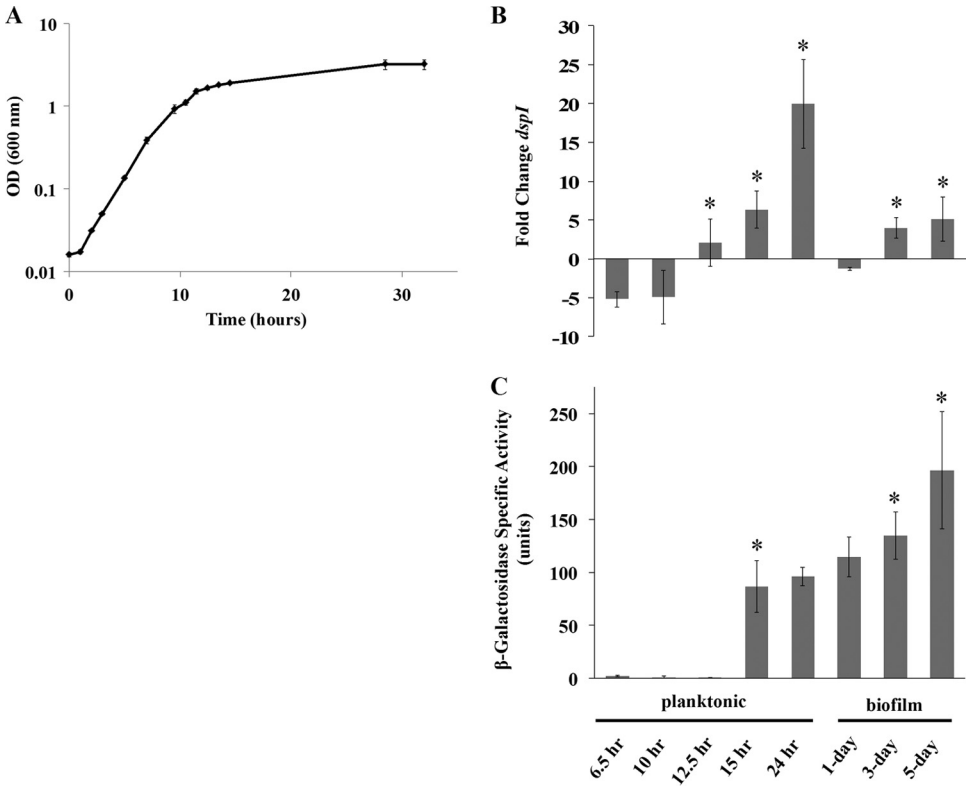

FIG 5 Expression and transcript abundance levels of *dspI* in planktonic and biofilm cells. (A) Growth curve of *P. aeruginosa* PA14 in LB medium. The curve represents the average of 3 replicates. The error bars indicate standard deviations. (B) Fold change in *dspI* mRNA levels in *P. aeruginosa* planktonic and biofilm cells compared to lag phase planktonic cells. Experiments were performed in triplicate. (C) Transcriptional reporter fusion assay for *dspI* expression in *P. aeruginosa* wild-type 6.5-h-, 10-h-, 12.5-h-, 15-h-, and 24-h-old planktonic cells and 1-day-, 3-day-, and 5-day-old biofilm cells. The values indicated by asterisks differ significantly from the values of the preceding growth phase ($P < 0.05$).

mine whether *dspI* promoter activity supported the finding of increasing *dspI* transcript levels with increasing cell density. The β-galactosidase activity of the *dspI* reporter construct was determined for planktonic cells at 6.5 h, 10 h, 12.5 h, 15 h, and 24 h and for biofilm cells at 1 day, 3 days, and 5 days. β-Galactosidase activity was also monitored by bright-field and fluorescence microscopy to determine when and where in the biofilm *dspI* promoter activity occurred. The β-galactosidase specific activity of 6.5-h, 10-h, and 12.5-h planktonic cells was below the level of detection but increased significantly in 15-h and 24-h cells (Fig. 5B and 6). Cell numbers in the images in Fig. 6 do not reflect the actual cell density in the sample. Similarly, β-galactosidase specific activity increased throughout biofilm development, with the highest level observed at 5 days (Fig. 5B). Microscopic observation of biofilm cells carrying the *dspI* reporter revealed β-galactosidase activity as early as 1 h after attachment to a glass substratum, with continued expression though 6 days of growth (Fig. 7). Individual cell reporter activity was not observed to be location specific within the biofilm. Control biofilms carrying the *lacZ* transcriptional reporter without an upstream *dspI* promoter did not show fluorescence at the single-cell level (see Fig. S3 in the supplemental material). Detectable fluorescence in cell clusters at 3 and 5 days was likely due to either autofluorescence of the cells or readthrough of RNA polymerase into the *lacZ* structural gene downstream from the *attB* integration site of the chromosome.

DISCUSSION

The structures of many fatty acid signals have been elucidated; however, the synthase genes for these signals are in many cases not identified. For those fatty acid signals whose synthase has been identified, all have been shown to be dependent on enoyl-CoA hydratase enzymes encoded by *rpfF* or *rpfF*-like homologs. In *X. campestris*, mutation of *rpfF* abolishes DSF production and results in reduced virulence of the plant pathogen. The gene *rpfF* is encoded by the *rpf* operon, which also includes the genes *rpfC* (sensor kinase) and *rpfG* (response regulator) (4).

Homologs of RpfF have been identified in *B. cenocepacia* (6), *X. oryzae* pv. *oryzae* (10), *X. fastidiosa* (18), *S. maltophilia* (13), and *X. axonopodis* pv. *glycines* (20). Thus, synthesis of fatty acid signaling molecules appears to be widely conserved. A BLAST search (www.pseudomonas.com) revealed homologs of RpfF (greater than 35% identity) in over 10 *Pseudomonas* species, indicating that production of small fatty acid signaling molecules may be widespread among members of the genus. Here, we report that DspI is a previously uncharacterized enoyl-CoA hydratase/isomerase that is required for production of the communication molecule *cis*-DA in *P. aeruginosa* (3). DspI is homologous (>30%) to the synthase RpfF in *X. campestris*, *X. oryzae*, *S. maltophilia*, and *X. fastidiosa*, as well as the synthase Bcam0581 in *B. cenocepacia* (Fig. 7A).

DspI is a putative member of the crotonase superfamily (Fig. 4A), which includes enzymes that catalyze the reversible addition

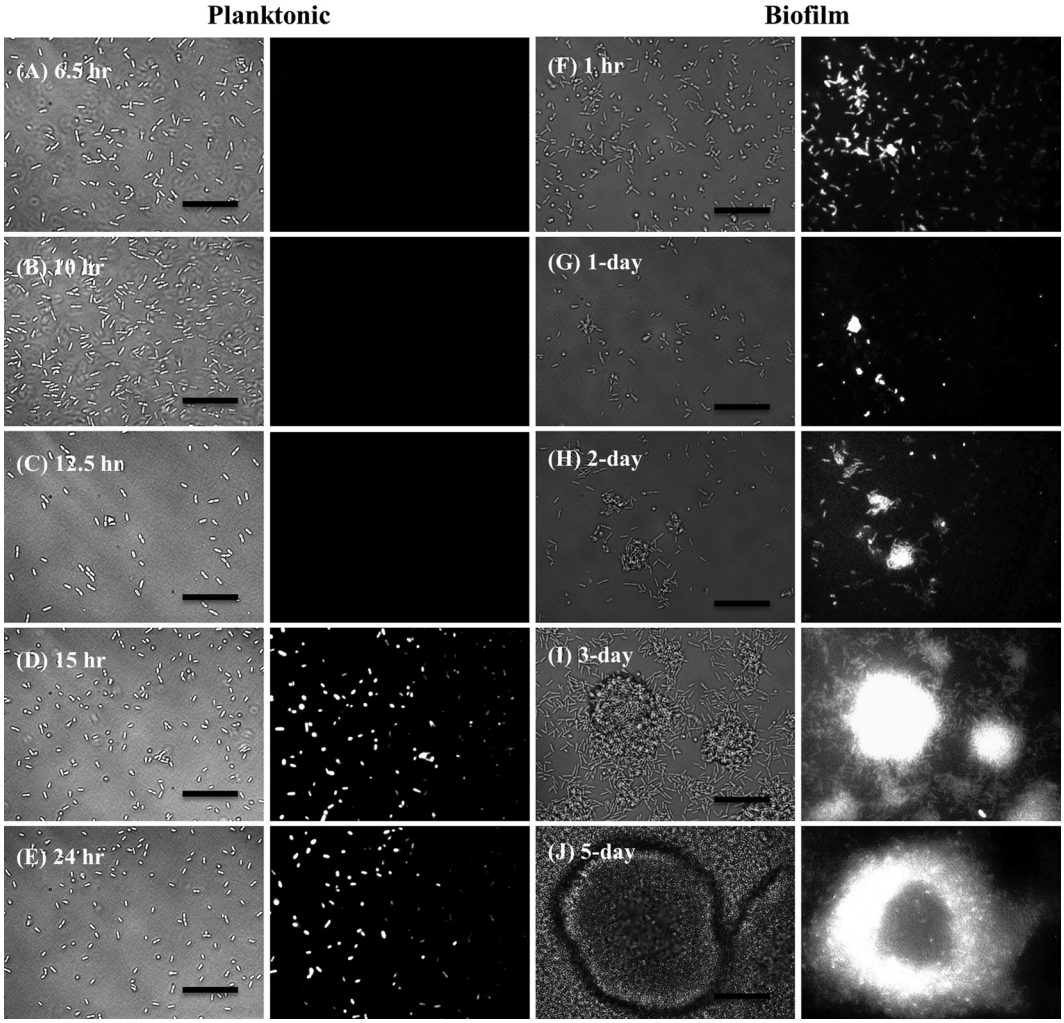

FIG 6 Microscopic analysis of *dspI* transcriptional-reporter activity during planktonic and biofilm growth. *P. aeruginosa* PA14 harboring a *dspI-lacZ* reporter construct was grown in batch or continuous culture in medium supplemented with MUG. The indicated planktonic (A to E) and biofilm (F to J) conditions are shown (bright-field images [left] and fluorescent cells displaying β-galactosidase activity [right]). Scale bars, 20 μm.

of water to α,β-unsaturated enoyl-CoA thioesters. Previous work has determined that rat mitochondrial enoyl-CoA hydratase contains two conserved catalytic glutamate residues, Glu^{144} and Glu^{164}, that are required for complex formation between the enzyme, a catalytic water, and the bound substrate at the active site (43–45). Sequence alignment of DspI with rat mitochondrial enoyl-CoA hydratase (NCBI accession number CAA34080) reveals that Glu^{144} and Glu^{164} align with Glu^{126} and Glu^{146} of DspI, supporting the role of DspI as a putative enoyl-CoA hydratase (Fig. 7B). These catalytic Glu residues are also conserved in RpfF of *X. campestris*, and mutation of either Glu residue abolished DSF synthesis (46).

Recently, Reddy et al. (47) identified a putative active site for the RpfF protein in *X. oryzae* pv. *oryzae*, which elucidated 29 amino acid residues involved in ligand binding: Leu^{84}, Gly^{85}, Gly^{86}, Leu^{88}, Phe^{91}, Ile^{95}, Tyr^{106}, Ala^{107}, Cys^{110}, Val^{111}, Leu^{136}, Gly^{137}, Gly^{138}, Glu^{141}, Pro^{160}, Glu^{161}, Leu^{163}, Leu^{164}, Leu^{166}, Pro^{168}, Gly^{169}, Met^{170}, Thr^{255}, Trp^{258}, Aal^{262}, Leu^{265}, Thr^{272}, Met^{273}, and Leu^{276}. Interestingly, the catalytic Glu^{144} and Glu^{164} residues for enoyl-CoA hydratase activity are included among those predicted to be involved in the active site (Fig. 7A). An alignment with *X. oryzae* RpfF reveals that *P. aeruginosa* DspI contains 15/29 of the predicted active-site amino acid residues, indicating that these are related enzymes that bind similar substrates and produce structurally related products (Fig. 7A).

It has been shown that mutation of *rpfC* results in increased DSF production and a significant increase in *rpfF* transcription (24, 48). This indicates that DSF detection by RpfC results in negative regulation of *rpfF*. This is in contrast to other quorum-sensing (QS) signaling systems, in which signal detection exhibits transcriptional positive feedback on the signal synthase. For example, in the *P. aeruginosa* QS LasR/I system, the 3-oxo-C_{12}-homoserine lactone ($3OC_{12}$-HSL) autoinducer molecule is produced by the LasI acylhomoserine lactone (AHL) synthase (49). Transcription of the *lasI* gene is positively regulated when the LasR regulator is bound to the signal, $3OC_{12}$-HSL (50). Interestingly, in *P. aeruginosa*, we have found no evidence of the *cis*-DA signal autoregulating the expression of its cognate synthase gene, *dspI*. Addition of synthetic *cis*-DA to late-exponential-stage planktonic cultures resulted in less than a 2-fold change in *dspI* transcript

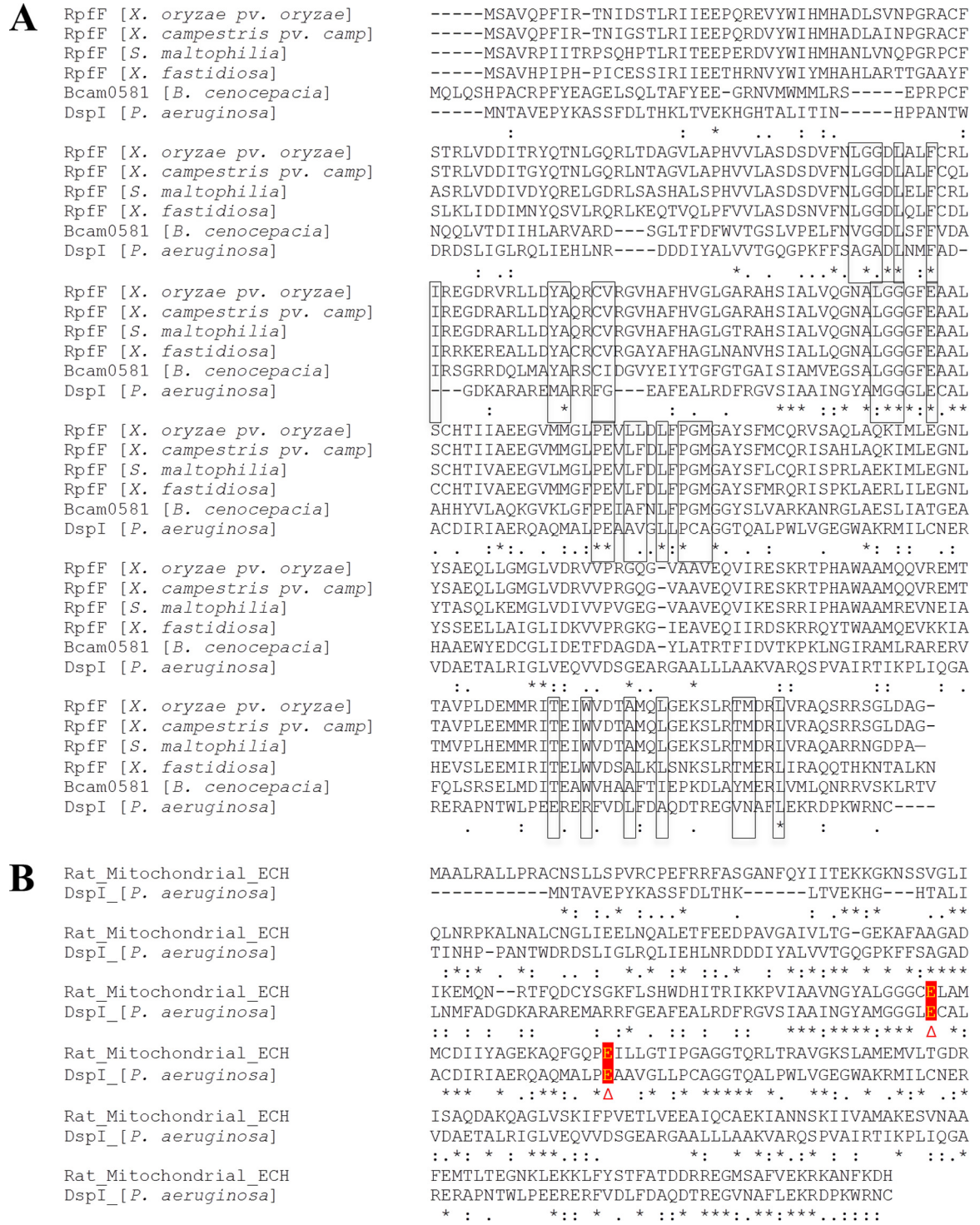

FIG 7 Multiple-sequence alignment of DspI, RpfF homologs, and rat mitochondrial enoyl-CoA hydratase. The sequences were obtained from the NCBI (http://www.ncbi.nlm.nih.gov/) and were aligned using ClustalW. Fully conserved (*), strongly conserved (:), and weakly conserved (.) amino acid residues are indicated. (A) The 29 amino acid residues of the predicted ligand binding site for RpfF in *X. oryzae* pv. *oryzae* are boxed (47). DspI contains 15 out of 29 conserved amino acid residues of the predicted DSF ligand binding site of RpfF. (B) Conserved glutamate residues at the enoyl-CoA active site of rat mitochondrial enoyl-CoA hydratase, Glu^{144} and Glu^{164}, align with Glu^{126} and Glu^{146} of DspI (shaded in red and indicated by triangles).

levels. These results do not support the idea that autoregulation of *cis*-DA synthesis occurs at the transcriptional level.

We have previously demonstrated the role of *cis*-DA as an autoinducer of biofilm dispersion in *P. aeruginosa* and that dispersion of mature biofilms is inducible by the exogenous addition of naturally or synthetically produced *cis*-DA (3). However, the full range of phenotypes regulated by this signaling molecule in *P. aeruginosa* has not been characterized. Recently, Feinbaum et al.

have shown that production of the virulence factor pyoverdine is reduced in *P. aeruginosa* when the gene PA14_54640 (*dspI*) is mutated (51). These mutants were also shown to be defective in swarming motility, a phenotype inversely correlated with biofilm formation (51). Together, these findings suggest that loss of *cis*-DA-induced dispersion may be associated with reduced pathogenicity and loss of swarming motility.

The discovery that DspI is required for *cis*-DA production has important implications for the future characterization of *cis*-DA signal transduction in *P. aeruginosa*. A two-component regulatory system for signal transduction of *cis*-DA has not yet been identified; however, several homologs of the DSF two-component regulatory system, RpfC/G, exist in *P. aeruginosa*. Elucidation of the signal transduction of *cis*-DA poses a significant challenge, considering that the *P. aeruginosa* genome encodes many predicted sensor kinase and response regulator proteins (63 and 64, respectively). A *dspI* mutant strain in which *cis*-DA production is abrogated yet that still disperses upon exogenous addition of *cis*-DA, may be a useful tool for future work to characterize *cis*-DA signal transduction- and dispersion-related phenotypes, including acute virulence and antimicrobial tolerance.

ACKNOWLEDGMENTS

We thank Karin Sauer, Olga Petrova, and Tim Lowenstein for their valuable assistance and for the use of their laboratory facilities. We also thank Allison Ferreira, Courtney Kleeschulte, Joycy Samson, and Ian Silverman for their contributions to this work.

This study was supported in part by NIH grant 1 R15 AI094485-01 2011.

REFERENCES

1. **Davies DG.** 1999. Regulation of matrix polymer in biofilm formation and dispersion, p 93–112. *In* Wingender J, Neu TR, Flemming H-C (ed), Microbial extrapolymeric substances, characterization, structure and function. Springer-Verlag, Berlin, Germany.
2. **Sauer K, Camper AK, Ehrlich GD, Costerton JW, Davies DG.** 2002. *Pseudomonas aeruginosa* displays multiple phenotypes during development as a biofilm. J. Bacteriol. **184:**1140–1154.
3. **Davies DG, Marques CNH.** 2009. A fatty acid messenger is responsible for inducing dispersion in microbial biofilms. J. Bacteriol. **191:**1393–1403.
4. **Barber CE, Tang JL, Feng JX, Pan MO, Wilson TJG, Slater H, Dow JM, Williams P, Daniels MJ.** 1997. A novel regulatory system required for pathogenicity of *Xanthomonas campestris* is mediated by a small diffusible signal molecule. Mol. Microbiol. **24:**555–566.
5. **Wang LH, He Y, Gao Y, Wu JE, Dong YH, He C, Wang SX, Weng LX, Xu J-L, Tay L, Fang RX, Zhang LH.** 2004. A bacterial cell-cell communication signal with cross-kingdom structural analogues. Mol. Microbiol. **51:**903–912.
6. **Boon C, Deng Y, Wang LH, He Y, Xu JL, Fan Y, Pan SQ, Zhang L-H.** 2008. A novel DSF-like signal from *Burkholderia cenocepacia* interferes with *Candida albicans* morphological transition. ISME J. **2:**27–36.
7. **Vílchez R, Lemme A, Ballhausen B, Thiel V, Schulz S, Jansen R, Sztajer H, Wagner-Döbler I.** 2010. *Streptococcus mutans* inhibits *Candida albicans* hyphal formation by the fatty acid signaling molecule *trans*-2-decenoic acid (SDSF). Chembiochem **11:**1552–1562.
8. **Beaulieu ED, Ionescu M, Chatterjee S, Yokota K, Trauner D, Lindow S.** 2013. Characterization of a diffusible signaling factor from *Xylella fastidiosa*. mBio **4:**e00539–00512. doi:10.1128/mBio.00539-12.
9. **Fouhy Y, Scanlon K, Schouest K, Spillane C, Crossman L, Avison MB, Ryan RP, Dow JM.** 2007. Diffusible signal factor-dependent cell-cell signaling and virulence in the nosocomial pathogen *Stenotrophomonas maltophilia*. J. Bacteriol. **189:**4964–4968.
10. **He YW, Wu J, Cha JS, Zhang LH.** 2010. Rice bacterial blight pathogen *Xanthomonas oryzae* pv. *oryzae* produces multiple DSF-family signals in regulation of virulence factor production. BMC Microbiol. **10:**187.
11. **Ryan RP, Fouhy Y, Garcia BF, Watt SA, Niehaus K, Yang L, Tolker-Nielsen T, Dow JM.** 2008. Interspecies signalling via the *Stenotrophomonas maltophilia* diffusible signal factor influences biofilm formation and polymyxin tolerance in *Pseudomonas aeruginosa*. Mol. Microbiol. **68:**75–86.
12. **Deng Y, Wu J, Eberl L, Zhang LH.** 2010. Structural and functional characterization of diffusible signal factor family quorum-sensing signals produced by members of the *Burkholderia cepacia* complex. Appl. Environ. Microbiol. **76:**4675–4683.
13. **Huang TP, Lee Wong AC.** 2007. Extracellular fatty acids facilitate flagella-independent translocation by *Stenotrophomonas maltophilia*. Res. Microbiol. **158:**702–711.
14. **Dow JM, Crossman L, Findlay K, He YQ, Feng JX, Tang JL.** 2003. Biofilm dispersal in *Xanthomonas campestris* is controlled by cell-cell signaling and is required for full virulence to plants. Proc. Natl. Acad. Sci. U. S. A. **100:**10995–11000.
15. **He YW, Xu M, Lin K, Ng YJ, Wen CM, Wang LH, Liu ZD, Zhang HB, Dong YH, Dow JM, Zhang LH.** 2006. Genome scale analysis of diffusible signal factor regulon in *Xanthomonas campestris* pv. *campestris*: identification of novel cell-cell communication-dependent genes and functions. Mol. Microbiol. **59:**610–622.
16. **He YW, Wang C, Zhou L, Song H, Dow JM, Zhang LH.** 2006. Dual signaling functions of the hybrid sensor kinase RpfC of *Xanthomonas campestris* involve either phosphorelay or receiver domain-protein interaction. J. Biol. Chem. **281:**33414–33421.
17. **Ryan RP, McCarthy Y, Andrade M, Farah CS, Armitage JP, Dow JM.** 2010. Cell-cell signal-dependent dynamic interactions between HD-GYP and GGDEF domain proteins mediate virulence in *Xanthomonas campestris*. Proc. Natl. Acad. Sci. U. S. A. **107:**5989–5994.
18. **Chatterjee S, Wistrom C, Lindow SE.** 2008. A cell-cell signaling sensor is required for virulence and insect transmission of *Xylella fastidiosa*. Proc. Natl. Acad. Sci. U. S. A. **105:**2670–2675.
19. **Chatterjee S, Sonti RV.** 2002. *rpfF* mutants of *Xanthomonas oryzae* pv. *oryzae* are deficient for virulence and growth under low iron conditions. Mol. Plant Microbe Interact. **15:**463–471.
20. **Thowthampitak J, Shaffer BT, Prathuangwong S, Loper JE.** 2008. Role of *rpfF* in virulence and exoenzyme production of *Xanthomonas axonopodis* pv. *glycines*, the causal agent of bacterial pustule of soybean. Phytopathology **98:**1252–1260.
21. **Ryan RP, McCarthy Y, Watt SA, Niehaus K, Dow JM.** 2009. Intraspecies signaling involving the diffusible signal factor BDSF (*cis*-2-dodecenoic acid) influences virulence in *Burkholderia cenocepacia*. J. Bacteriol. **191:**5013–5019.
22. **Deng Y, Boon C, Eberl L, Zhang LH.** 2009. Differential modulation of *Burkholderia cenocepacia* virulence and energy metabolism by the quorum-sensing signal BDSF and its synthase. J. Bacteriol. **191:**7270–7278.
23. **McCarthy Y, Yang L, Twomey KB, Sass A, Tolker-Nielsen T, Mahenthiralingam E, Dow JM, Ryan RP.** 2010. A sensor kinase recognizing the cell-cell signal BDSF (*cis*-2-dodecenoic acid) regulates virulence in *Burkholderia cenocepacia*. Mol. Microbiol. **77:**1220–1236.
24. **Slater H, Alvarez-Morales A, Barber CE, Daniels MJ, Dow JM.** 2000. A two-component system involving an HD-GYP domain protein links cell-cell signalling to pathogenicity gene expression in *Xanthomonas campestris*. Mol. Microbiol. **38:**986–1003.
25. **Cohen-Bazire G, Sistrom WR, Stanier RY.** 1957. Kinetic studies of pigment synthesis by non-sulfur purple bacteria. J. Cell Physiol. **49:**25–68.
26. **Liberati NT, Urbach JM, Miyata S, Lee DG, Drenkard E, Wu G, Villanueva J, Wei T, Ausubel FM.** 2006. An ordered, nonredundant library of *Pseudomonas aeruginosa* strain PA14 transposon insertion mutants. Proc. Natl. Acad. Sci. U. S. A. **103:**2833–2838.
27. **Kaneko Y, Thoendel M, Olakanmi O, Britigan BE, Singh PK.** 2007. The transition metal gallium disrupts *Pseudomonas aeruginosa* iron metabolism and has antimicrobial and antibiofilm activity. J. Clin. Invest. **117:**877–888.
28. **Becher A, Schweizer HP.** 2000. Integration-proficient *Pseudomonas aeruginosa* vectors for isolation of single-copy chromosomal *lacZ* and *lux* gene fusions. Biotechniques **29:**948–950, 952.
29. **Mohr CD, Leveau JHJ, Krieg DP, Hibler NS, Deretic V.** 1992. AlgR-binding sites within the *algD* promoter make up a set of inverted repeats separated by a large intervening segment of DNA. J. Bacteriol. **174:**6624–6633.
30. **Mohr CD, Hibler NS, Deretic V.** 1991. AlgR, a response regulator controlling mucoidy in Pseudomonas aeruginosa, binds to the FUS sites of the algD promoter located unusually far upstream from the mRNA start site. J. Bacteriol. **173:**5136–5143.

31. **Figurski DH, Helinski DR.** 1979. Replication of an origin-containing derivative of plasmid RK2 dependent on a plasmid function provided *in trans*. Proc. Natl. Acad. Sci. U. S. A. **76:**1648–1652.
32. **Hoang TT, Schweizer HP.** 1997. Fatty acid biosynthesis in *Pseudomonas aeruginosa*: cloning and characterization of the *fabAB* operon encoding beta-hydroxyacyl-acyl carrier protein dehydratase (FabA) and beta-ketoacyl-acyl carrier protein synthase I (FabB). J. Bacteriol. **179:**5326–5332.
33. **Heydorn A, Nielsen AT, Hentzer M, Sternberg C, Givskov M, Ersbøll BK, Molin S.** 2000. Quantification of biofilm structures by the novel computer program COMSTAT. Microbiology **146:**2395–2407.
34. **Davies DG, Parsek MR, Pearson JP, Iglewski BH, Costerton JW, Greenberg EP.** 1998. The involvement of cell-to-cell signals in the development of a bacterial biofilm. Science **280:**295–298.
35. **Allegrucci M, Sauer K.** 2007. Characterization of colony morphology variants isolated from *Streptococcus pneumoniae* biofilms. J. Bacteriol. **189:**2030–2038.
36. **Allegrucci M, Sauer K.** 2008. Formation of *Streptococcus pneumoniae* non-phase-variable colony variants is due to increased mutation frequency present under biofilm growth conditions. J. Bacteriol. **190:**6330–6339.
37. **Petrova OE, Sauer K.** 2009. A novel signaling network essential for regulating *Pseudomonas aeruginosa* biofilm development. PLoS Pathog. **5:**e1000668. doi:10.1371/journal.ppat.1000668.
38. **Southey-Pillig CJ, Davies DG, Sauer K.** 2005. Characterization of temporal protein production in *Pseudomonas aeruginosa* biofilms. J. Bacteriol. **187:**8114–8126.
39. **Miller J.** 1972. Experiments in molecular genetics, p 352–355. Cold Spring Harbor Laboratory, Cold Spring Harbor, NY.
40. **Davies DG, Geesey GG.** 1995. Regulation of the alginate biosynthesis gene *algC* in *Pseudomonas aeruginosa* during biofilm development in continuous culture. Appl. Environ. Microbiol. **61:**860–867.
41. **Davies DG, Chakrabarty AM, Geesey GG.** 1993. Exopolysaccharide production in biofilms: substratum activation of alginate gene expression by *Pseudomonas aeruginosa*. Appl. Environ. Microbiol. **59:**1181–1186.
42. **Stoodley P, Wilson S, Hall-Stoodley L, Boyle JD, Lappin-Scott HM, Costerton JW.** 2001. Growth and detachment of cell clusters from mature mixed-species biofilms. Appl. Environ. Microbiol. **67:**5608–5613.
43. **Bahnson BJ, Anderson VE, Petsko GA.** 2002. Structural mechanism of enoyl-CoA hydratase: three atoms from a single water are added in either an E1cb stepwise or concerted fashion. Biochemistry **41:**2621–2629.
44. **Engel CK, Mathieu M, Zeelen JP, Hiltunen JK, Wierenga RK.** 1996. Crystal structure of enoyl-coenzyme A (CoA) hydratase at 2.5 angstroms resolution: a spiral fold defines the CoA-binding pocket. EMBO J. **15:**5135–5145.
45. **Engel CK, Kiema TR, Hiltunen JK, Wierenga RK.** 1998. The crystal structure of enoyl-CoA hydratase complexed with octanoyl-CoA reveals the structural adaptations required for binding of a long chain fatty acid-CoA molecule. J. Mol. Biol. **275:**847–859.
46. **Cheng Z, He Y-W, Lim SC, Qamra R, Walsh MA, Zhang L-H, Song H.** 2010. Structural basis of the sensor-synthase interaction in autoinduction of the quorum sensing signal DSF biosynthesis. Structure **18:**1199–1209.
47. **Reddy VS, Kumar YN, Raghavendra A, Sowjenya G, Kumar S, Ramyasree G, Reddy GR.** 2012. In silico model of DSF synthase RpfF protein from *Xanthomonas oryzae* pv. *oryzae*: a novel target for bacterial blight of rice disease. Bioinformation **8:**504–507.
48. **An S-Q, Febrer M, McCarthy Y, Tang D-J, Clissold L, Kaithakottil G, Swarbreck D, Tang J-L, Rogers J, Dow JM, Ryan RP.** 2013. High-resolution transcriptional analysis of the regulatory influence of cell-to-cell signaling reveals novel genes that contribute to *Xanthomonas* phytopathogenesis. Mol. Microbiol. **88:**1058–1069.
49. **Pearson JP, Pesci EC, Iglewski BH.** 1997. Roles of *Pseudomonas aeruginosa las* and *rhl* quorum-sensing systems in control of elastase and rhamnolipid biosynthesis genes. J. Bacteriol. **179:**5756–5767.
50. **Seed PC, Passador L, Iglewski BH.** 1995. Activation of the *Pseudomonas aeruginosa lasI* gene by LasR and the *Pseudomonas* autoinducer PAI: an autoinduction regulatory hierarchy. J. Bacteriol. **177:**654–659.
51. **Feinbaum RL, Urbach JM, Liberati NT, Djonovic S, Adonizio A, Carvunis A-R, Ausubel FM.** 2012. Genome-wide identification of *Pseudomonas aeruginosa* virulence-related genes using a *Caenorhabditis elegans* infection model. PLoS Pathog. **8:**e1002813. doi:10.1371/journal.ppat.1002813.